Scour around Spur Dyke: Recent Advances and Future Researches

Hao ZHANG and Hajime NAKAGAWA

Synopsis

Scour is a common phenomenon in river engineering and a challenging problem for hydraulic research. Scour may bring human either benefits or disasters depending on whether the scour process is well understood and effectively managed. Investigation on scour around spur dyke has a long history and still receives much attention to date. This paper provides background knowledge and research prospect on this topic. The paper is organized mainly in three parts. The first part presents a state-of-the-art on related researches such as the flow structure, estimation formulae for equilibrium scour depth, temporal and spatial variation of scour and scour around grouped spur dykes. After that, recent advances in numerical modeling techniques are presented, including the principle ideas, governing equations and solution methods. Finally, possible avenues for future researches are suggested.

Keywords: spur dyke, scour, recent advances, future researches

1. Introduction

Spur dykes are typical man-made hydraulic structures and are widely constructed in alluvial rivers all over the world. Spur dykes are generally built perpendicular or at an angle to the channel bank or revetment, protruding into the watercourse. Historically, spur dykes were constructed to prevent channel banks or levees from erosion by diverting away approaching flows, to improve river navigation conditions by deepening the main channel bed or to secure water supply and agriculture irrigation by maintaining suitable flow discharge and water level. Nevertheless, aesthetic and environmental impacts of spur dykes have attracted much attention since several decades before. Nowadays, spur dykes are also considered as a promising measure to enhance diversities of channel morphologies and riverine eco-systems.

Spur dykes may be classified into various types. According to structure permeability, spur dykes are generally categorized into two types: impermeable and permeable (Fig.1a). Impermeable spur dykes are built of local soil, stones, gravels, rocks or gabions, while permeable ones usually consist of one or several rows of timber, bamboo, steel or reinforced concrete piles. An impermeable spur dyke blocks and defects the river flow, while a permeable one allows water to pass through it at a reduced velocity. Based on submergence conditions, submerged and non-submerged spur dykes are distinguished (Fig.1b). In general, the submerged condition is not desirable for impermeable spur dykes since the overtopping flow may cause severe erosion and damage. Spur dykes may be classified as attracting, deflecting or repelling spur dykes according to their inclination as shown in Fig.1c. An attracting spur dyke points downstream and attracts the flow towards its head and thus to the bank. In contrast, a repelling spur dyke inclines in upstream direction and diverts the flow away from itself. The spur dyke normal to the flow is a deflecting one. It diverts the flow at its head and results in a wake zone behind it. Classification of spur dykes may also be made according to their appearances (Fig.1d). Due to the importance of the

head as will be discussed later, spur dykes are designed with various appearances mainly in terms of the shape of the head. Apart from a straight spur dyke, alternatives may include a mole-head, L-head, T-head or hockey-shaped one.

Typical flow

Impermeable   Permeable

(a) Permeability

Water surface

Submerged   Non-submerged

(b) Submergence

Typical flow

Attracting   Deflecting   Repelling

(c) Inclination

Flow direction

Straight Mole-head L-head T-head Hockey-shaped
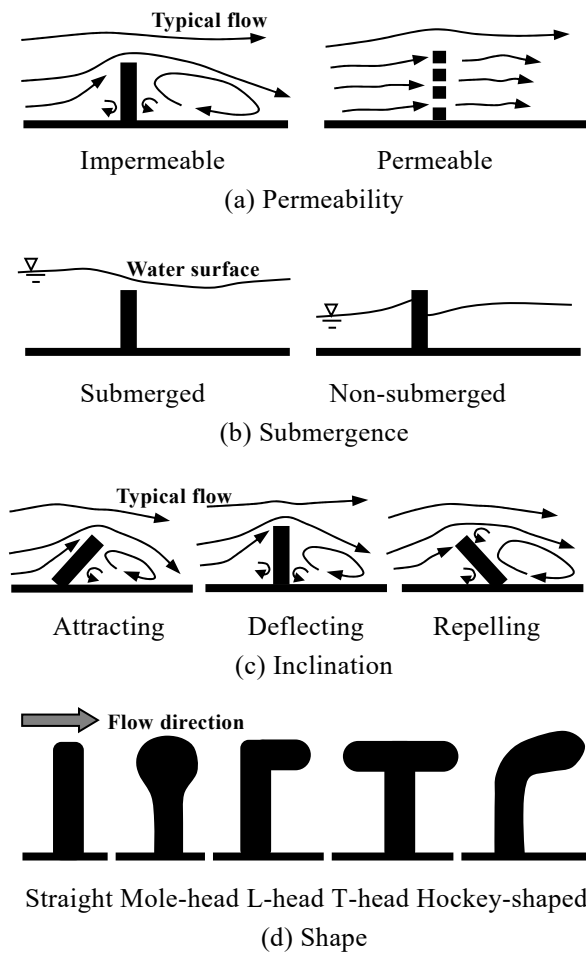
(d) Shape

Fig.1 Classification of spur dykes

Protruding of a structure such as a spur dyke to a channel leads to changes on the flow patterns and bed configurations. These changes usually initiate a scour process, involving turbulent flow, sediment transport and erodible boundaries. This process is a dynamic feedback process. A clear understanding and a scientific interpretation of this process are a prior for successful design and sustainable management of hydraulic structures. Consequently, tremendous amount of researches have been conducted over the years in laboratory experiments, numerical simulations and field measurements. As is known, scour is a localized lowering of channel bed due to the imbalance of sediment transport. The scour occurring at a spur dyke is generally divided into three categories: general scour, constriction

scour and local scour. General scour takes place on a channel bed as a result of sediment transport irrespective of whether or not a spur dyke is there. Constriction scour arises from the narrowing of the watercourse by the presence of the spur dyke. Local scour results directly from the impact of the spur dyke on the local flow pattern. It is noticed that local scour is usually superimposed on constriction scour. Based on the sediment transport mode by the approaching flow, local scour is either a clear-water scour or a live-bed scour. Clear-water scour refers to conditions when the bed material upstream of the scour area is at rest, i.e. the near-bed shear stress u_* some distance away from the spur dyke is not greater than the critical shear stress u_{*c} for the initiation of particle movement. Live-bed scour takes place when the near-bed shear stress is generally greater than the critical one and the flow induces general sediment transport. Clear-water scour and live-bed scour are usually differentiated in conventional analyses of local scour. The temporal variation of the maximum scour depths under clear-water scour and live-bed scour conditions are schematically shown in Fig.2.

Dynamic equilibrium scour depth

Scour depth

Live-bed scour

Equilibrium scour depth

Clear-water scour

t
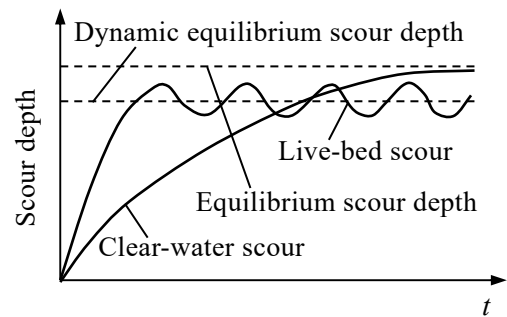
(a) Temporal variation of local scour
(after Chabert and Engeldinger, 1956)

Clear-water peak

Live-bed peak

Averaged scour depth

Live-bed scour

Clear-water scour

0   1   2   3   4 u_*/u_{*c}
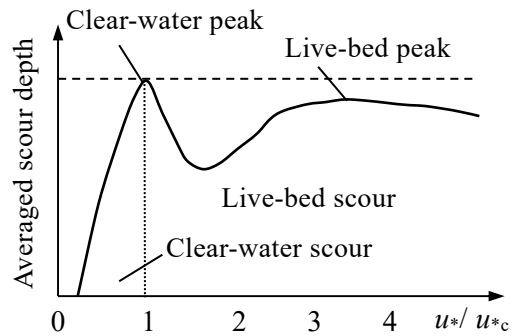
(b) Local scour against shear stress
(after Chiew, 1984)

Fig.2 Sketch of clear-water and live-bed scour

In general, clear-water scour may be divided into several stages: initial stage, development stage, stabilization stage and equilibrium stage. The scour develops quickly at initial and development stages and shows insignificant changes at the stabilization stage. An equilibrium stage is reached finally, which usually takes a longer time compared with a live-bed scour. In case of live-bed scour, the scour increases rapidly with time and then fluctuates about a mean value in response to the passages of bed forms (Fig.2a). Although the near-bed shear stress under live-bed scour condition is larger than that under clear-water scour condition, the maximum scour depth in the former case is not necessarily larger than that in the latter one. Scour occurs when the near-bed shear stress is larger than a critical value (Fig.2b). With the increasing of the near-bed shear stress, the scour depth at the equilibrium stage increases. A peak value occurs when the near-bed shear stress equals to the critical shear stress. This peak is called a clear-water peak. The scour depth decreases from the clear-water peak with the development of bed forms and reaches a minimum value when the deepest bed forms take place. The scour depth increases to a new peak with the further increasing of the near-bed shear stress. This peak is named a transition flat bed peak (or live-bed peak), at which stage bed forms disappear and more flow energy contributes to the scour process. When the bed forms appear again at still higher near-bed shear stress and dissipate some of the flow energy, the scour depth decreases again.

Excessive scour is one of the major causes for failures of spur dykes. On the other hand, the pool-riffle morphologies, as consequences of scour, provide new river amenities and important habitats for riverine species. Therefore, a balance should be well maintained to achieve the maximum beneficial effects and still afford an effective control of the scour. This necessitates a deep insight into the associated problems and underlying processes, together with advanced prediction methods and tools if available. This paper firstly presents a review on up-to-date knowledge and conventional approaches. After that, recent advances, especially in numerical modeling, are discussed. Avenues for future researches are suggested at the final part.

2. Scour around a single spur dyke

2.1 Flow structure around a spur dyke

An insight into the nature of the flow is a prerequisite for the understanding of the scour process. In general, the flow initiates and controls the scour process. The flow past a spur dyke is generally complex and this complexity increases with the development of the scour hole.

(1) Flow separation and vortex shedding

The flow past the spur dyke may be divided into three zones: a main flow zone from the head of the spur dyke to the opposite side of the channel, a wake zone behind the spur dyke and a mixing zone in-between them (Fig. 3).

In the main flow zone, the velocity is accelerated. Molinas et al. (1998) reported in their experimental research that the velocity at the spur dyke head might be increased up to 1.5 times the approaching flow velocity, depending on the flow conditions and spur dyke protrusion ratios. Ho et al. (2007) presented similar results when they investigated the flow around different impermeable spur dykes with both experimental and numerical methods.
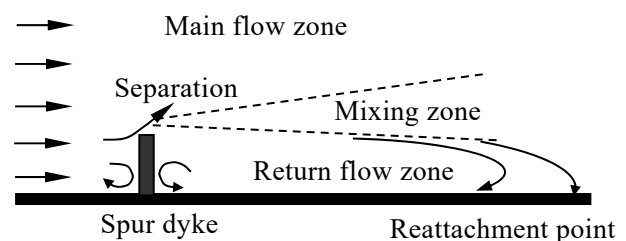

Fig.3 Typical flow around spur dyke

The wake zone may be further subdivided into a return flow zone and a reattachment zone. The return flow zone is generally characterized by two eddies of different rotating direction and size. A small eddy is near to the spur dyke, the centre of which locates at a distance almost equal to the spur dyke length L. A larger eddy is at the downstream of the small one, whose centre locates a distance of about $6L$ away from the spur dyke. The reattachment zone is an area where the separated flow reattaches the channel bank downstream of the spur dyke. According to Chen and Ikeda (1997), the length of the reattachment zone covers a distance of

around 6*L* and locates over the range from 11*L* to 17*L*. The reattachment zone is usually simplified into a point for the convenience of analyses. At this point, the time-averaged velocity is zero. But it should be kept in mind that the instantaneous reattachment point fluctuates back and forth. For impermeable spur dykes, Ouillon and Dartus (1997) reported that the location of the reattachment point was 11.5*L* in experiments and 10.7*L* with a numerical model study. With a depth averaged numerical model, Liu et al. (1994) found that the angle of inclination showed more remarkable effects than the shape of the spur dyke on the reattachment point. Moreover, the location of the reattachment point is the farthest for a repelling spur dyke compared with a deflecting or an attracting one with the same effective length. Ho et al. (2007) investigated the separation length (distance between the spur dyke and the reattachment point) behind a single spur dyke with different permeability. They found that the separation length decreases with the increasing of spur dyke permeability. For 0% (impermeable), 20% and 80% permeability, the separation length is 12.5*L*, 5.7*L* and 1.8*L*, respectively. Furthermore, it wa noticed that the wake zone shrank with the development of scour hole according to the authors' experimental studies. The flow structure on the water surface entirely changed from a flat bed to a scoured bed. The change of the local bed configuration and the development of the 3D vortex systems were responsible for this phenomenon.

The vortex shedding in the mixing zone is an important aspect of the flow field. By measuring the water level fluctuations along the centerline of the migrating vortices, Chen and Ikeda (1997) found that there were clear periodic water level fluctuations. These fluctuations showed obvious phase difference between two consecutive measuring points, which suggested a strong coherency between them. The correlation coefficient was determined with FFT (Fast Fourier Transformation) method for each pair of time series of water surface fluctuations. The lag time when the correlation coefficient took a peak was considered as the migration time of a vortex. It was found that the migration velocity of the vortices was kept to be constant, which was a little larger than the mean

flow velocity. The vortices shedding from the spur dyke merged with each other as they migrated downstream. As a result, there were increases in both length scale and time scale of the vortices.

(2) Flow structure in the scour area

The flow in local scour generally shows obvious 3D characteristics. This 3D flow may be divided into several components. In front of the spur dyke, there exists a bow wave near the water surface and a downflow towards the channel bed due to the stagnation of approaching flow. As the result of the flow separation, a horse-shoe vortex develops in the local scour hole and a wake vortex system forms behind the spur dyke. A schematic diagram of the flow and local scour at the longitudinal section passing the spur dyke head is shown as below.
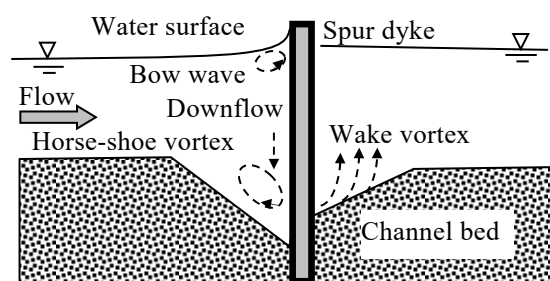

Fig.4 Typical flow in a scour hole

The authors have investigated the flow structure in a scour hole with two sets of electro-magnetic velocimetries in a laboratory flume. The hydraulic condition is given in Zhang and Nakagawa (2008). The local scour geometry is shown in Fig.5, which is obtained with a laser displacement meter. The mean velocity profiles at typical cross-sections are shown in Fig.6 and Fig.7. From these figures, one may have a clear image on the complex vortex systems in the proximity of the spur dyke.
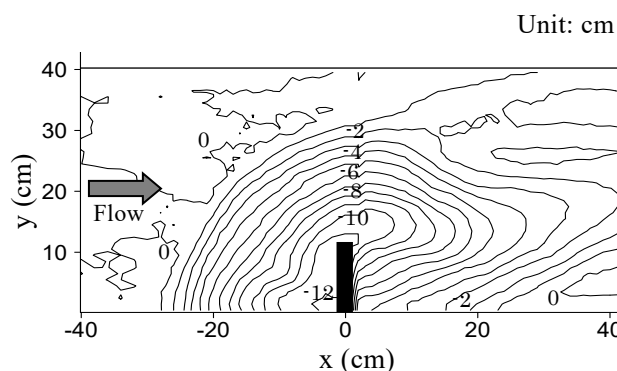
Unit: cm

Fig.5 Scour around an impermeable spur dyke

(a) Transverse section x=-4cm

(b) Transverse section x=0cm
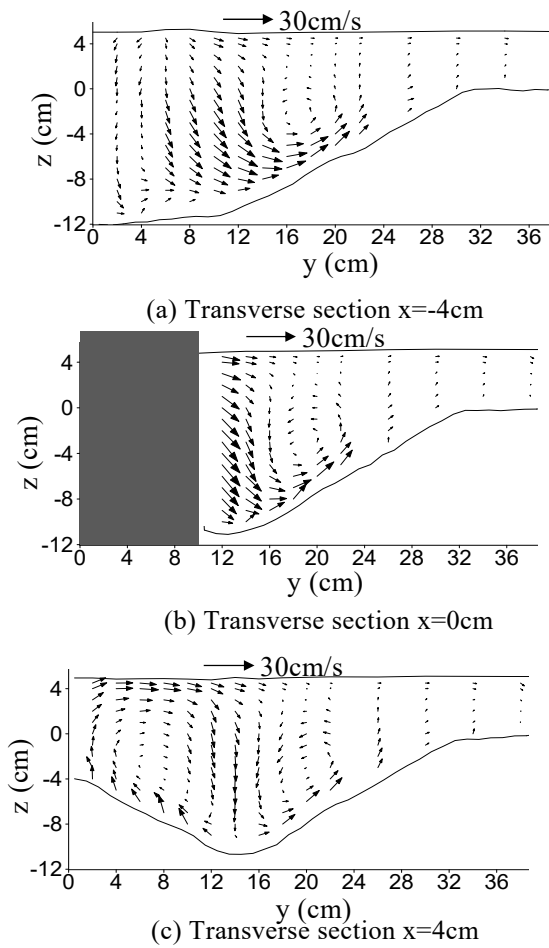

(c) Transverse section x=4cm

Fig.6 Transverse flow velocity in a scour hole

2.2 Parameters related to scour at a spur dyke

The scour depth depends on a lot of parameters characterizing the fluid, the bed sediment, the flow condition, the channel geometry and the spur dyke structure. Researches have been conducted in the literature to identify the roles of these parameters with laboratory experiments, numerical simulations or field measurements. However, there remain many disputed points on which there is a lack of general agreement. Since a spur dyke is very similar to an abutment in many aspects, results obtained for bridge abutments are considered to be applicable for spur dykes as well. Based on existing researches, the aforementioned parameters and their influences on the scour process are detailed as follows.

(1) Parameters related to the fluid

Parameters include the fluid density ρ, the kinematic viscosity υ, the gravitational acceleration g and the temperature T. The change of these parameters is generally assumed to be insignificant in a specific hydraulic experiment or an actual river

reach. However, it should be noticed that the effect of these parameters might become important in some cases. For example, the change of the viscosity due to temperature variation may affect the sediment threshold condition as well as the development of bed forms and thus the flow field. According to a series of laboratory experiments conducted in the authors' group relating to scour around spur dykes (e.g. Zhang, 2005), it is found that experiments in the winter season takes a longer time than those in summer times in order to arrive at an equilibrium condition due to the differences in water temperature.
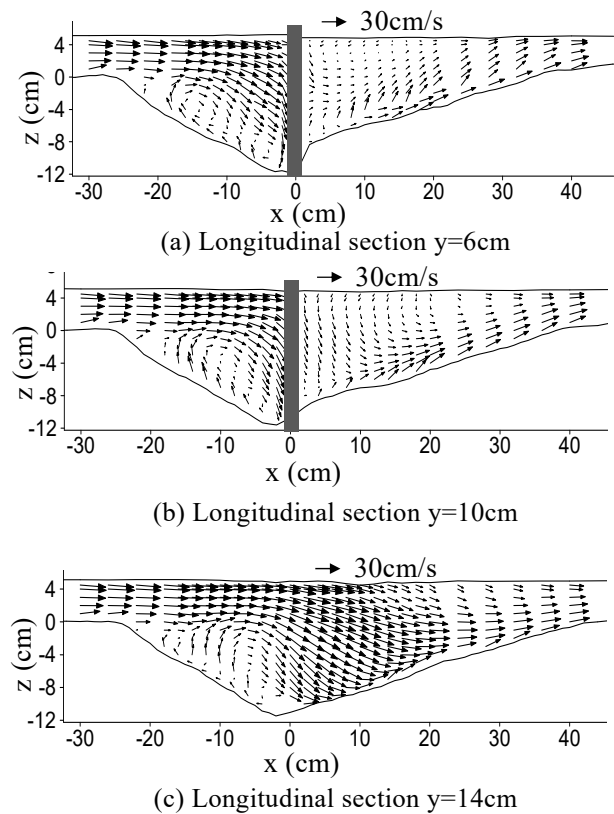

(a) Longitudinal section y=6cm

(b) Longitudinal section y=10cm

(c) Longitudinal section y=14cm

Fig.7 Longitudinal flow velocity in a scour hole

(2) Parameters related to bed sediment

Parameters include the particle density ρ_s, the angle of repose φ, the mean diameter d, grain size distribution, cohesiveness and bed consolidation. Studies concerning the latter two parameters are still in its infant and are not detailed here.

Laursen (1960) has stated that the maximum scour depth was affected by sediment size under clear-water scour but not under live-bed scour. But it was argued to be curious by many researchers. Garde et al. (1961) did experiments with four sand

sizes in range 0.29mm to 2.25mm under live-bed scour condition and found that the sediment size influenced both the rate of scour and the maximum scour depth. He included the sediment size in a drag coefficient and incorporated it into a semi-empirical equation for the estimation of scour depth. Gill (1972) reported that the rate of scour development of the fine sand was higher than that of the coarse sand according to his experiments with two sediment sizes (d=0.914mm and d=1.52mm). For the same value of near-bed shear stress in the approaching flow area, fine sediments resulted in greater scour depth. The reduction in scour depth for relatively large sediment might be due to large particles impeding the erosion process at the base of the scour hole and dissipating some of the flow energy in the erosion zone. However, the coarse sand was scoured deeper than the fine sand for the same value of τ/τ_c, in which τ= near-bed shear stress in the approaching flow area and τ_c =critical shear stress of bed material. Raudkivi and Ettema (1983) believed that the relative grain size defined by L/d had more meaning compared with the grain size d itself to analyze the effect of sediment size on scour depth. The scour depth was independent of the sediment size if the relative grain size was large enough. Melville (1997) agreed with them and included the relative grain size, rather than the grain size itself, in his prediction formula.

The geometric standard deviation σ_g, generally defined as $\sigma_g = \sqrt{d_{84}/d_{16}}$ is an important parameter for the analysis of grain size distribution. It is commonly accepted that the sediment may be considered uniform if σ_g <1.4 and nonuniform else. Armor layer may form on the channel bed and in the scour hole during the scour process in nonuniform sediment bed. It has significant effect on the maximum scour depth. Melville and Sutherland (1988) pointed out the existence of a limiting armor condition which represented the coarsest or most stable armored bed for a given bed material and could be characterized by a mean velocity u_{ca}. Each sediment had a unique value of u_{ca}, dependent on the sediment size and grading. For nonuniform sediment bed, the clear-water peak would be replaced by an armor peak. The critical flow velocity at the armor peak u_a was determined using u_a=0.8u_{ca}. u_a marked the transition from

clear-water scour to live-bed scour in nonuniform sediment bed and was equivalent to u_c for uniform sediment. For velocities less than u_a, armoring occurred and the scour depth was limited accordingly. Beyond u_a, the armoring diminished and the scour depth was reasonably constant irrespective of σ_g at the live-bed peak.

Raudkivi and Ettema (1983) found that the maximum clear-water equilibrium scour depth, for sediment with a shape factor near one, depended on σ_g. They proposed a practical relation to estimate the equilibrium scour depth at a bridge pier in nonuniform sediment bed in terms of the geometric standard deviation as follows.

$$\frac{d(\sigma_g)}{D} = K_\sigma \frac{d}{D} \tag{1}$$

where D= bridge pier diameter and K_σ= coefficient which depended on σ_g, giving by a diagram.

According to experimental studies conducted by Dey and Barbhuiya (2004), the scour depth at an abutment with an armor-layer in clear-water scour condition under limiting stability of surface particles was always greater than that without an armor-layer for the same bed sediments.

(3) Parameters related to flow condition

The approaching flow depth and mean velocity are two important parameters. According to experimental studies carried out by Gill (1972) and others, it may be concluded that the maximum scour depth increased at a decreasing rate with the increasing in approaching flow depth. The scour depth increased proportionately with the flow depth for shallow flows and was independent of flow depth in case of deep flows. An explanation was that the bow wave that formed in front of the spur dyke interfered with the down flow and horseshoe vortex in shallow flows and the two had opposite senses of rotation. With the increasing of flow depth, the interference reduced and became insignificant eventually. The flow velocity, being incorporated in the shear stress in many researches, deserves special attention. According to the ratio of the flow velocity and the critical flow velocity for sediment threshold, scour may be classified as clear-water scour and live-bed scour as has been mentioned in the previous contexts. Since there are

significant differences between the two classes of scour as discussed before, it is important to consider them separately. In general, the effect of flow conditions is not discussed separately. They usually come with, saying, the dimension of the spur dyke structure and the critical velocity or shear stress for sediment threshold/armoring.

(4) Parameters related to geometry of channel

Rectangular channel has been assumed in most of the researches and the channel width is the only parameter which needs to be considered. But an actual river generally has various shapes. A complex channel geometry poses great challenges not only because there are many difficulties in characterizing its dimensions but also because it puts forward new problems on how to adequately quantify other parameters such as the water depth, the velocity and the effective length of spur dyke.

Sturm and Janjua (1994) studied the scour around an abutment in a compound channel. The abutment was situated in the floodplain setting well back from the edge of the main channel. The main channel was treated as fixed-bed channel, while the floodplain was covered with sediment, clear-water scour occurring at the abutment. A discharge contraction ratio was introduced to account for the compound channel effects. This ratio represented the redistribution of flow between the main channel and the floodplain as the flow passed through the abutment contraction. A more systematic study was conducted by Melville (1995). The study was limited to the case of an abutment spanning the floodplain and extending into the main channel.

Type 1   Type 2

Type 3a   Type 3b
Fig.8 Scour types in compound channel
(after Melville, 1995)

Melville (1995) suggested three types of scour in idealized compound channels as shown in Fig. 8. Type1 applied to an abutment spanning a well-defined channel without floodplain. In Type2, the abutment spanned the floodplain and extended into the main channel. In Type3, the abutment spanned only part of the floodplain. Type3 was further divided into two cases: the abutment in Type3a extended only partly across the floodplain while terminated at about the edge of the main channel in Type3b. The effect of the channel geometry on the scour depth was represented by a multiplying factor K_G as will be discussed in the latter contexts. The K_G was defined as the ratio of the scour depth at an abutment in a compound channel to a scour depth at an abutment in a corresponding rectangular channel. In general, K_G was a function of the size, shape, roughness of the main channel and the floodplain. Cardoso and Bettess (1999) studied Type3 abutment scour with a set of laboratory experiments. Their results were in conformity with Melville's suggestion that scour at abutments on floodplains could be approximated by scour in rectangular channels if an imaginary boundary (sketched in Type3a, Fig.5) was assumed separating the flows in the main channel and the floodplain. From this point, Type3 scour might be treated as special cases of Type1 scour. However, they observed that the time to equilibrium was shorter, by up to a factor of 7, when the scour hole extended into the main channel than when the scour hole was confined entirely to the floodplain.

(5) Parameters related to spur dyke structure

Parameters include the size, shape, alignment and permeability of the spur dyke.

The effective length L is usually used in the analysis of scour around spur dykes instead of the actual length. The effective length is defined as the projected length of a spur dyke, i.e. the length perpendicular to the flow. Therefore, spur dykes of different alignment extending the same lateral distance into the flow have different actual lengths. According to the ratio of L/h, Melville (1995) classified bridge abutments as short, intermediate length and long abutments. Melville (1995) stated that for a long abutment, the scour depth was independent of the abutment length.
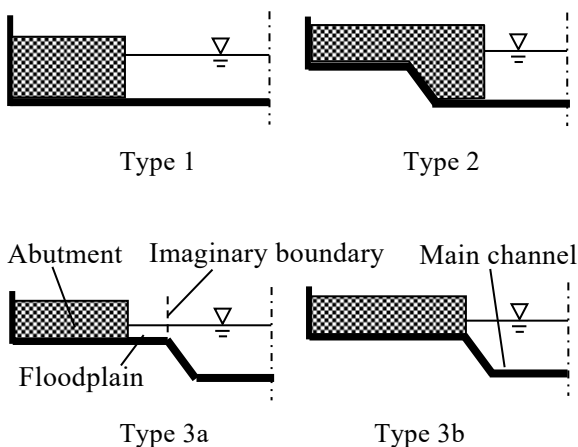
The shape of the spur dyke has a significant effect on the local flow structure and hence the scour process. A streamlined body is usually expected to reduce the drag exerted by the flow and to reduce the size of the wake and general flow disturbances. A vertical wall abutment causes greater scour depth in comparison with other types. For a long abutment, Melville (1992) argued that the shape of the abutment became unimportant.

The inclination angle of the spur dyke to the approaching flow significantly influences the scour depth. Early researches carried out by Garde et al. (1961) suggested that the maximum scour depth was greatest for a spur dyke with an inclination angle of 90° and smaller for all other inclinations upstream and downstream. But this was disputed by Tison (1962), who argued that the greatest maximum scour depth was recorded for an upstream spur dyke inclination, followed by the 90° and the downstream ones with evident experimental data. Tison (1962) also gave explanations on the observed variations of maximum scour depth with the inclination angle using a simple theory, in which the importance of the vertical driving motion on the scour development was emphasized. For short abutment, Melville (1992) stated that the effect of the inclination angle could be ignored.

The permeability of spur dyke also affects the scour depth significantly. The scour depth and area at an impermeable spur dyke are remarkably larger than those at a permeable one (Zhang, 2005). Yeo (2007) conducted a series of experiments to investigate the local scour at spur dykes with permeability ranged from 0% to 80%. Normalizing the maximum scour depth at a spur dyke with the maximum scour depth at an impermeable spur dyke, he found that the dimensionless scour depth decreased with the increasing of the structure permeability. The relation was nearly linear. The locations of the maximum scour depth were almost the same in both impermeable and permeable cases. However, the scour area was concentrated at the head of the impermeable spur dyke, whereas the channel bed in the proximity of the spur dyke was significantly scoured in all permeable cases. Zhang (2005) observed that the scour hole had a V-shape along the axis of the permeable spur dyke.

A typical scour at a permeable spur dyke with 50% permeability is given below (Zhang and Nakagawa, 2008). The hydraulic condition for this experiment is the same as that in Fig.5, except that the impermeable spur dyke is replaced with a permeable one. Compared with the contour in Fig.5, it is found that the maximum scour depth here is less than half of that in the impermeable case.
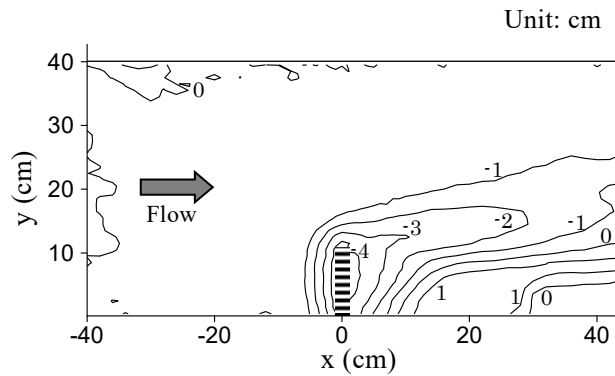
Unit: cm

Fig.9 Scour around a permeable spur dyke

2.3 Equilibrium scour depth

In order to estimate the maximum scour depth, a lot of relations and formulae have been developed. Basically, these relations or formulae are grouped into four categories: (1) regime approach relating the scour depth to the increased discharge intensity; (2) dimensional analysis approach based on field or experiment data; (3) analytical or semi-analytical approach and (4) probabilistic approach.

(1) Regime approach

In the regime approach, scour depth is a function of the flow discharge at the contracted section. Based on Lacey's regime formula, Inglis (1949) proposed a scour prediction equation.

$$d_s + h = 0.47 k_i (Q/f)^{1/3} \qquad (2)$$

where d_s= equilibrium scour depth; h= water depth from initial bed; f=silt factor, is equal to $1.76\sqrt{d}$; d= mean diameter of sediment; Q= regime discharge and k_i= amplification factor for local scour depth, depending on the type of obstructions. Another representative relation is that presented by Ahmad (1953), having the form as

$$d_s + h = k_a q^{2/3} \qquad (3)$$

where k_a= constant depending on the flow intensity and the inclination angle of the spur dyke and q= discharge per unit width in the contracted section.

This kind of approach suffers from an inherent drawback as the regime concept originates from the analysis of general scour whereas the mechanism of scour around a spur dyke is quite different from that of general scour. As a consequence, some dominant factors for maximum scour depth are not taken into account such as the dimension of the spur dyke and the mode of sediment transport.

(2) Dimensional analysis

Using dimensional analysis and experimental and/or field data, a significant amount of formulae are developed. As has been mentioned before, there are a lot of parameters entering the problem. In practice, those parameters are generally not directly converted to dimensionless variables. Instead, they are carefully selected and combined to work together, resulting in variables such as the Froude number, the dimensionless shear stress and so on.

Garde et al. (1961) correlated the scour depth with dimensionless parameters as

$$(d_s + h)/h = f(\alpha, \theta, Fr, C_D) \tag{4}$$

where $\alpha=(B-L)/B$, the opening ratio, in which B is the width of the channel; θ = angle of inclination of spur dyke with the direction of approaching flow; $F_r = u/\sqrt{gh}$, the Froude number, in which u is the approaching flow velocity and C_D= drag coefficient of sediment, defined as

$$C_D = 4(s-1)gd/(3\rho w_s^2) \tag{5}$$

where $s=\rho_s/\rho$ and w_s= settling velocity of sediment.

Assuming constant relative density of sediment and absence of viscous effect, Melville (1992) proposed the following expression

$$\frac{d_s}{h} = f\left(\frac{u^2}{gd}, \frac{L}{h}, \frac{d}{h}, \sigma_g, Sh, Al, SG\right) \tag{6}$$

where Sh, Al = parameters describing the shape and alignment of the abutment and SG= parameter describing the effects of lateral distribution of flow and cross-sectional shape of the approach channel.

Sturm and Janjua (1994), on the other hand, introduced the following expression when they investigate abutment scour in a compound channel.

$$d_s/h = f(F_r, F_{rc}, M) \tag{7}$$

where F_r= approaching Froude number in the floodplain, defined by the velocity and depth upstream of the end of the abutment; F_{rc}= critical value of the approaching Froude number for initiation of motion and M= discharge contraction ratio, defined as the ratio of the discharge approaching section through the opening width to the total discharge.

The equations derived from dimensional analysis are evaluated with laboratory experimental data and/or field data. A lot of empirical formulae are then developed. Some formulae are developed for clear-water scour, some are for live-bed scour, and some are intended to include both. The estimation formula proposed by Melville (1997) includes extensive data from bridge piers and abutments. It has been frequently cited in the literature. This formula is written as

$$d_s = K_{hL}K_I K_d K_s K_\theta K_G \tag{8}$$

where K= empirical expressions accounting for various influences on scour depth, termed K-factors hereafter. K_{hL} = factor for flow depth and abutment length; K_I = factor for flow intensity; K_d = factor for sediment size; K_s = factor for abutment shape; K_θ = factor for abutment alignment and K_G = factor for channel geometry. The K-factors are considered individually and are evaluated by fitting envelope curves to existing data for bridge foundations.

Melville (1997) suggested following estimation methods for the factors of K_{hL} and K_I.

$$K_{hL} = \begin{cases} 2L & if & \dfrac{L}{h} < 1 \\ 2\sqrt{hL} & if & 1 < \dfrac{L}{h} < 25 \\ 10h & if & \dfrac{L}{h} > 25 \end{cases} \tag{9}$$

$$K_I = \begin{cases} 1 & if & \dfrac{u-(u_a-u_c)}{u_c} \geq 1 \\ \dfrac{u-(u_a-u_c)}{u_c} & if & \dfrac{u-(u_a-u_c)}{u_c} < 1 \end{cases} \tag{10}$$

in which, the critical velocity may be related to the critical frictional velocity via the logarithmic form of the velocity profile, i.e.

$$\frac{u_c}{u_{*c}} = 5.75\log\left(5.53\frac{h}{d}\right) \qquad (11)$$

$$\frac{u_{ca}}{u_{*ca}} = 5.75\log\left(5.53\frac{h}{d_a}\right) \qquad (12)$$

The critical shear velocities u_{*c}, u_{*ca} are determined from the sediment size d and the median armor size d_a, using the Shields diagram or other relations. The median armor size of the sediment is found with an empirical expression given by Chin et al. (1994)

$$d_a = d_{max}/1.8 \qquad (13)$$

where d_{max}= the maximum particle size of the nonuniform sediment material.

The expression in Eq. (10) indicates that the scour depth is approximately proportional to the flow intensity under clear-water scour but is independent of flow velocity under live-bed scour.

The factor related to sediment size K_d has the following form. In case of nonuniform sediment, the d is replaced with d_a.

$$K_d = \begin{cases} 1.0 & if \quad \dfrac{L}{d} > 25 \\ 0.57\log\left(2.24\dfrac{L}{d}\right) & if \quad \dfrac{L}{d} \le 25 \end{cases} \qquad (14)$$

Selecting the vertical wall abutment as the primary shape, the shape factor K_s for typical shape of abutment is given in Table 1.

Because the shape effects become unimportant at longer abutments, Melville (1997) recommended using the adjusted shape factor K_s^* in the prediction formula as follows.

$$K_s^* = \begin{cases} K_s & if \quad \dfrac{L}{h} \le 10 \\ K_s + 0.667(1-K_s)(\dfrac{L}{10h}-1) & if \quad 10 < \dfrac{L}{h} < 25 \\ 1.0 & if \quad \dfrac{L}{h} \ge 25 \end{cases} \qquad (15)$$

Selecting the right angle as reference, the alignment factor K_θ is given in Table 2.
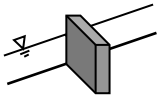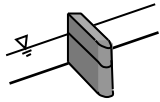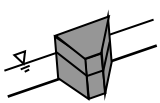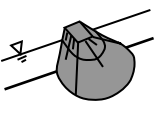
Table 1 Shape factors (after Melville, 1992)

Model	Shape	K_s
	Vertical wall	1.00
	Semicircular ended	0.75
	Wing-wall	0.75
	Spill-through with slope horizontal:vertical 0.5:1	0.60
	horizontal:vertical 1:1	0.50
	horizontal:vertical 1.5:1	0.45

Table 2 Alignment factors (after Melville, 1992)

θ	30	60	90	120	150
K_θ	0.90	0.97	1.00	1.06	1.08

Melville (1992) recommended that the alignment factor be applied to longer abutments only and gave the adjusted alignment factor K_θ^* as

$$K_\theta^* = \begin{cases} K_\theta & if \quad \dfrac{L}{h} \ge 3 \\ K_\theta + (1-K_\theta)(1.5-\dfrac{L}{2h}) & if \quad 1 < \dfrac{L}{h} < 3 \\ 1.0 & if \quad \dfrac{L}{h} \le 1 \end{cases} \qquad (16)$$

Finally, the effect of the channel geometry for a compound channel is given by

$$K_G = \sqrt{1 - \frac{B^*}{B}\left[1 - \left(\frac{h^*}{h}\right)^{5/3}\frac{n^*}{n}\right]} \qquad (17)$$

where B, B^*= width of the main channel and the floodplain, respectively; h^*= water depth in the floodplain; n, n^*= Manning's roughness coefficient for the main channel and floodplain, respectively.

With the all the K-factors known, the maximum scour depth is readily estimated.

(3) Analytical and semi-analytical approach

The dimensional analysis approach has been successful to predict local scour in many laboratory flumes. However, this kind of approach does not

include any treatment to model the physical process unique to the scour phenomenon. Hence, the applicability and generality of this kind of method are quite questionable, especially in prototype scales. In early investigations, Laursen (1960, 1963) developed formulae, based on scour at long contraction, for clear-water and live-bed scour depths at vertical-wall abutments as follows.

For live-bed scour (Laursen, 1960)

$$\frac{L}{h} = 2.75\left(\frac{d_s}{h}\right)\left[\left(\frac{1}{r}\frac{d_s}{h}+1\right)^{7/6}-1\right] \tag{18}$$

For clear-water scour (Laursen, 1963)

$$\frac{L}{h} = 2.75\left(\frac{d_s}{h}\right)\left\{\left[\left(\frac{1}{r}\frac{d_s}{h}\right)+1\right]^{7/6}\Big/\left(\frac{u_{*p}}{u_{*c}}\right)-1\right\} \tag{19}$$

where u_{*p}= shear stress associated with sediment particles; r= ratio of scour depth at abutment to scour depth in equivalent long contraction. It is assumed that r=11.5 for live-bed scour and r=12 for clear-water scour.

Based on the premise that the flow obstruction and the subsequent increases in bed shear stress due to the projection of abutment are responsible for the scour, Lim (1997) developed a semi-empirical formula for clear-water scour

$$d_s/h = K_s\left(0.9X_a - 2\right) \tag{20}$$

where K_s= shape factor as given in Table1, and $X_a = \tau_{*ca}^{-0.375}F_{da}^{0.75}(d/h)^{0.25}[0.9(L/h)^{0.5}+1]$, where F_{da}= sediment densimetric Froude number based on d_a

$$F_{da} = u/\sqrt{(s-1)gd_a} \tag{21}$$

After introducing a generalized bed-load transport relation, Lim and Cheng (1998) extended Lim's work to live-bed scour conditions as

$$\left(1+\frac{d_s}{2h}\right)^{4/3} = \frac{1+1.2\sqrt{\dfrac{L}{h}}}{\sqrt{\dfrac{u_{*c}^2}{u_*^2}+\left(1-\dfrac{u_{*c}^2}{u_*^2}\right)\left(\dfrac{L\tan\phi}{d_s}+1\right)^{2/3}}} \tag{22}$$

(4) Probabilistic approach

There are many uncertainties during the estimation of the scour depth. Johnson and Dock (1998) classified the uncertainties into three groups: 1) model; 2) hydraulics and 3) parameters. The model uncertainty comes from the using of a model that may not be completely representative of the physical process. Hydraulic uncertainty is the result, for example, of attempting to estimate flow depth and velocity for a specific discharge at a particular location. Parameter uncertainty results from an inability to accurately access parameters and model coefficients required in the model.

Probabilistic approach for scour is still very few. In order to obtain a probabilistic scour depth, for example, Johnson and Dock (1998) suggested a working procedure using the Monte Carlo method. The procedure is as follows: 1) generate values for each of the random variables in a deterministic model; 2) estimate the scour depth from the deterministic model based on the generated random variables; 3) repeat *Procedure2* for *N* simulation cycles; 4) Calculate the mean and deviation for the *N* values of scour depth; 5) Obtain the distribution of the *N* values of scour depth.

2.4 Temporal variation of scour depth

The time required by a given discharge to scour to its full potential is generally much larger than the time for which it runs (Kothyari and Ranga Raju, 2001). Therefore, temporal variation of scour is of great significance, in particular to predict the scour in an actual river where the flow is unsteady and discharge changes rapidly.

Kothyari and Ranga Raju (2001) noticed that scour process around a spur dyke was similar to that around a pier except that the boundary layer effect induced by the channel wall might cause less scour in the spur dyke case. They introduced the concept of an analogous pier, the size of which was determined through an analysis of the drag force experienced by the pier and the spur dyke. Estimation formula for scour process around piers (Kothyari et al. 1992) was then used to predict the scour around a spur dyke. The model was verified under both clear-water and live-bed scour conditions. Coleman et al. (2003) presented an expression to predict the temporal variation of scour depth by determining a function relating the time-dependent scour depth to the equilibrium

scour depth. In case of uniform sediment and clear-water scour condition, an equation was proposed to evaluate the time to equilibrium scour, which was defined as the time required for the rate of scouring to reduce to 5% of the smaller of the spur dyke length L or the flow depth h in the succeeding $24h$ period.

Dey and Barbhuiya (2005) developed a model for the temporal variation of scour depth based on the concept of mass conservation of sediment particles, considering the horse-shoe vortex as the main agent for scouring and assuming a layer by layer scour process. Apart from other models, they obtained the temporal variation of scour depth by solving a differential equation instead of relating it to the equilibrium scour depth. The model was successfully applied to predict the scour process around short abutments of different shapes in uniform and non-uniform sediments under clear-water scour conditions.

2.5 Geometry of scour at a spur dyke

The volume and geometry of a scour hole is valuable for assessing the potential benefit to the aquatic habitat. Shields et al. (1995) documented significant increases in fish numbers, sizes, species and the area of aquatic habitat after the enlargement of local scour in a river restoration project. In the proximity of the historically built spur dykes along the Yodo River in Osaka, Japan, favorable environment for the growth and habitant of a variety of living things have also been observed. (Kinki Regional Development Bureau, MLIT, Japan 2002). Unfortunately, very few studies have been carried out on this subject to date.

Kuhnle et al. (1999, 2002) investigated the shape and volume of local scour around different types of spur dykes under different flow conditions with experimental methods. They plotted the topographic maps showing the geometries of the scour around spur dyke and suggested a simple prediction scheme for the area and volume of scour holes. In the prediction method, the maximum scour depth was predicted firstly based on Melville's relation as described before, and then the scour depth was converted to a volume using relations derived from experimental data. According to their reports, the overtopping ratio (approach flow depth

divided by spur dyke height) and the protrusion angle were two important parameters which affected the geometry of local scour. Larger overtopping ratios caused the region of maximum scour to shift toward channel bank and caused a secondary scour zone to form downstream of the spur dyke. Compared with deflecting and attracting spur dykes, repelling spur dykes generally resulted in maximum scour volume and minimum near-bank erosion.

Ishigaki and Baba (2004) reported an experimental study on the scour around deflecting and attracting spur dykes under submerged and non-submerged conditions. They pointed out that the deflecting spur dyke was more effective than the attracting one in protecting channel bank erosion, coinciding with the observations in Kuhnle et al (2002). Ishigaki and Baba (2004) also argued that scour holes occurred at the head of the deflecting spur dyke and located near the root of the attracting one in submerged conditions.

Typical scour holes around an impermeable and a permeable spur dyke under clear-water scour condition have been shown in Fig.5 and Fig.9, respectively.

3. Scour around grouped spur dykes

In order to improve the efficiency, spur dykes are generally organized in a group. A single spur dyke is not commonly observed in actual rivers. For a group of spur dykes, there are some new parameters that should be paid much attention, for example, the spacing between two consecutive spur dykes, termed embayment in this paper.

3.1 Main channel-embayment exchanges

The embayment between two consecutive spur dykes attracts a lot of attention nowadays mainly due to its environmental function, i.e. maintaining a wide variety of fauna and flora in the river system. The exchange process between the main channel and the embayment plays an important role in determining the effectiveness of spur dykes.

Nakagawa et al. (1995), Muto et al. (2000) and Zhang (2005) investigated the flow structure in rectangular embayments of different aspect ratios. The aspect ratio was defined as W/L, in which W

was the length of the embayment and *L* was the effective length of the spur dyke. They concluded that the aspect ratio determined the shape and stability of circulating flow induced in the embayment. An aspect ratio close to unity gave rise to a single circulation, whose center almost coincided with the geometrical center of the embayment. Larger aspect ratios resulted in two circulating flows. One was large and located in the downstream part of the embayment. Another one was small and emerged just behind the upstream spur dyke. The two circulations were in opposite direction. With extreme large aspect ratio of six, penetration of the main channel flow into the embayment would be observed as shown in Uijttewaal (1999). However, the two circulating flows remained in a relatively stable position.

The flow near an embayment is characterized by the generation of coherent vortex in-between the main channel and the embayment and free-surface oscillation inside it. Kimura and Hosoda (1997) investigated the two processes and their interactions with both experimental and numerical methods. According to their results, a large coherent vortex with subsequent small vortices took place periodically, consistent with that of the free surface oscillation. The temporal velocity variation might be decomposed into two components that were caused by the free surface oscillation and the shear instability in the mixing area. Due to the non-linear interaction between the shear instability and free surface oscillation, the vortex caused by the shear instability was amplified selectively. Once the vortex was amplified, the following vortices merged into the main circulation until next period started.

Uijttewaal et al. (2001) conducted physical scale model experiments in a 20m-long and 3m-wide channel with a series of embayments. According to their result, reducing the main channel velocity had no effect on the flow pattern in the embayment, whereas lowering the water level did. In the latter case, the effects of the bottom slope became more pronounced, shifting the centre of the circulation flow towards the main channel. Uijttewaal et al. (2001) also argued that the shape of the spur dyke was of minor importance for the exchange process.

Researches of Muto et al. (2000) and Uijttewaal et al. (2001) indicated that horizontal circulation was dominant in embayments under non-submerged conditions. Small-scale 3D turbulence played a minor role in the mass and momentum exchange process between the main channel and the embayment. Under submerged condition, however, Nakagawa et al. (1995) pointed out that vertical circulation was important according to their experimental study. Kimura et al. (2002) reported obvious vertical circulating flow in an embayment with numerical simulations, consistent with the original experimental data.

3.2 Scour caused by grouped spur dykes

(1) Main channel degradation

The degradation of the main channel caused by a group of spur dykes is generally treated as a long constriction scour. The reduction of the channel width due to the construction of spur dykes results in increases in near-bed shear stress and hence considerable scour within the constricted reach. Nevertheless, the main channel degradation caused by grouped spur dykes is slightly different from that of a solid long constriction due to the flow separation around the heads of spur dykes.
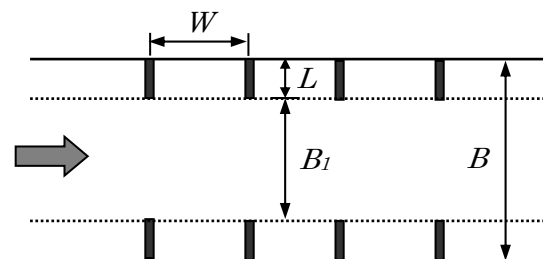

Fig. 10 Definition of factor λ

Michiue et al. (1984) and Suzuki (1989) suggested an equivalent constriction width by introducing a factor λ which modifies the constriction width caused by the construction of grouped spur dykes as λB_1 , where B_1 is the constriction width as sketched in Fig.10. From known values for the bed degradation in flume experiments and numerical computation, the factor λ is determined with a diagram. λ takes a value of 1.0 when aspect ratio approaches 0 or is between 4 and 8 and the spur dykes work almost the same as a long constriction. λ is larger than unity when the

aspect ratio is larger than 8 and takes a value of B/B_1 when the aspect ratio approaches infinity. That is, spur dykes work independently when the aspect ratio is very large. Furthermore, the main channel degradation is larger than that of a long constriction when the aspect ratio is between 0 and 4 (i.e. λ is less than unity). The suggested estimation formula for the main channel degradation Δz is as below.

$$\frac{\Delta z}{h} = \left(\frac{\lambda B_1}{B}\right)^{-4/7} - 1 + \frac{u^2}{2gh}\left[\left(\frac{\lambda B_1}{B}\right)^{-6/7} - 1\right] \qquad (23)$$

(2) Local scour around each spur dyke

Local scour varies with the location of the spur dyke in the group. In general, the scour depth at the head of the most upstream spur dyke (denoted as first spur dyke hereafter) is similar to that of a single one, whereas which far from the first spur dyke is different from a single one due to the influence of the neighboring spur dykes.

From experimental result, Suzuki (1989) and Zhang (2005) found that local scour holes showed insignificant changes from the 4th spur dyke. Suzuki (1989) suggested to estimate the maximum scour depth at the first spur dyke d_{s1} with any prediction formula for a single spur dyke as discussed before and proposed the following expression for the scour depth after the nth spur dyke d_{sc} in a group.

$$\frac{d_{sc}}{d_{s1}} = 0.07\frac{W}{L} + 0.14 \qquad (24)$$

(3) Morphological consequences of spur dykes

From the perspective of waterfront recreation and river environment, investigation on the main channel degradation or the local scour alone is far from enough. There is a great public demand on researches concerning diversity of river flow and channel morphology after the construction of spur dykes. It is expected that people might take full use of rivers' aesthetic and ecological values if spur dykes are effectively arranged.

Zhang (2005) and Zhang et al. (2005) studied the morphological consequences of a series of impermeable and permeable spur dykes in laboratory experiments. The permeable spur dykes have a permeability of 50%. The experiments were carried out under clear-water scour regime and last around 2 months in order to achieve the equilibrium condition. The bed deformation is shown in Fig. 11.

According to the experimental result, main channel degradation caused by the impermeable spur dykes was quite similar to that of the permeable ones. However, severe local scour took place at the most upstream pair of impermeable spur dykes, which had a potential to undermine the foundation of spur dykes. Local scour around other impermeable spur dykes was relatively smaller and was expected to provide suitable pool habitat for aquatic species. Considering the effect on the formation of pool-riffle morphology, Zhang et al. (2005) suggested to combine the impermeable and permeable spur dykes in a group. In order to prevent the channel bank from erosion by the return currents, an aspect ratio less than three was
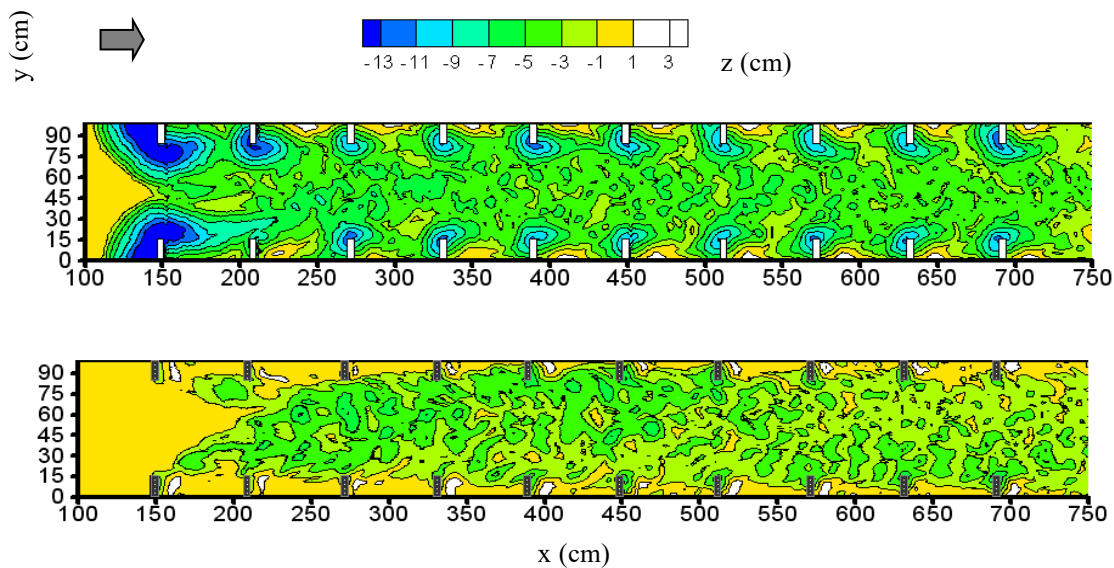

Fig. 11 Morphological consequences of grouped spur dykes (Impermeable, Top; Permeable, Bottom)

recommended by Zhang (2005) based on both experimental and numerical results.

Besides the permeability and the aspect ratio, orientation angle also plays an important role in the arrangement of spur dykes. Tominaga and Matsumoto (2006) investigated the pool-riffle morphology caused by grouped spur dykes with an angle to the channel bank under submerged flow conditions. For spur dyke groups inclined towards upstream, severe scour holes were observed around the heads of spur dykes and deposition regions occurred beside the channel bank. For spur dyke groups orienting downstream, front regions of spur dykes and area near the channel bank were significantly scoured. An alternate arrangement of spur dykes inclined towards upstream was satisfactory to create pool-riffle morphology.

4. Numerical modeling of scour at spur dyke

Conventional methods for scour prediction involve lots of empiricism, simplifications and uncertainties. It is quite risky to implement these methods in engineering practice if a deep insight is not assured into the problem to be solved. With the rapid development of CFD (Computational fluid dynamics) and computer sciences, more general and reliable approaches become attainable. Since scour is a localized degradation of channel bed due to imbalance of sediment transport, numerical models developed for sediment transport and bed deformation in alluvial channels could be applied to predict scour process. But generally it is not the fact in practice. Scour around spur dyke is a relatively local problem and necessitates the resolution of many local quantities. Unfortunately, local phenomena are commonly ignored or not well-resolved in general alluvial river models. Therefore, although alluvial river modeling has been presented in many literatures such as Cao and Carling (2001), it is still necessary to have a section to discuss the numerical modeling of scour around spur dyke, emphasizing on some unique aspects.

In general, three kinds of numerical modeling researches have been conducted in the past several decades: (1) numerical modeling of flow field with planar or unscoured bed (e.g. Mayerle et al., 1995; Ouillon and Dartus, 1997; Peng and Kawahara,

1998; Kimura et al., 2002; Nakagawa et al., 2004 and Ho et al., 2007); (2) numerical modeling of flow field with scoured bed (e.g. Marson et al., 2003; Tominaga and Matsumoto, 2006 and Teraguchi et al., 2008) and (3) numerical modeling of flow field and bed deformation with movable bed (e.g. Michiue and Hinokidani, 1992; Yoseef and Klaassen, 2002; Bhuiyan et al, 2004; Nagata et al., 2005; Zhang et al., 2006; Onda et al., 2007 and Zhang et al., 2008). The performances of existing numerical models are mostly evaluated according to researchers' preferences as well as verification data at hand. Some of these models are reported to well resolve the typical horseshoe vortex in the scour hole area (e.g. Marson et al., 2003 and Nagata et al., 2005) and some are concentrated on the reasonable reproduction of the reattachment length behind the spur dyke (e.g. Mayerle et al., 1995, Ouillon and Dartus, 1997 and Ho et al. 2007). Some are focused on the elaborateness of the turbulence model (e.g. Yossef and Klaassen, 2002) and some pay more attention on the sediment transport routines (e.g. Onda et al., 2007). It is noticed that reliable and detailed experimental data is still insufficient both in amount and in quality concerning the 3D flow and scour around spur dykes. Therefore, there is still a long way for the verification of numerical models. Moreover, in order to have a practicable model for actual use in river engineering, much space remains to improve the model elaborateness and cost-effectiveness.

4.1 General approach on scour modeling

Modeling the scour process, in essence, is the modeling of a strongly coupled system involving flow, sediment and morphology. Direct resolving this system is almost impossible to date and seems hardly attainable in near future. As an alternative, it is usually decoupled in the numerical modeling.
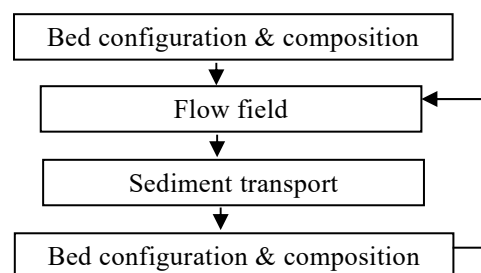
Fig. 12 Typical flow-chat of scour modeling

A typical flow chart for the simulation of scour at spur dyke is shown in Fig. 12. It is evident from Fig. 12 that a numerical model generally consists of three modules: a hydrodynamic module for the simulation of the flow field, a sediment module for the modeling of sediment transport and a bed variation module to account for the change of the bed topography and sediment composition.

4.2 Turbulent flow modeling

The LES (Large eddy simulation) based on the space-filtered Navier-Stokes equations experienced significant development in the past several decades. But its application is still confined in experimental fumes and is very limited in scour modeling. Full 3D modeling of flow of engineering interest is built on the RANS (Reynolds-averaged Navier-Stokes) equations. Particularly, the k-ε model is widely used, whose governing equations are written as

$$\frac{\partial u_i}{\partial x_i} = 0 \tag{25}$$

$$\frac{\partial u_i}{\partial t} + u_j \frac{\partial u_i}{\partial x_j} = f_i - \frac{1}{\rho}\frac{\partial p}{\partial x_i} + v\frac{\partial^2 u_i}{\partial x_j \partial x_j} + \frac{1}{\rho}\frac{\partial \tau_{ij}}{\partial x_j} \tag{26}$$

$$\frac{\partial k}{\partial t} + u_j \frac{\partial k}{\partial x_j} = \frac{\partial}{\partial x_j}\left[\left(v + \frac{v_t}{\sigma_k}\right)\frac{\partial k}{\partial x_j}\right] + G - \varepsilon \tag{27}$$

$$\frac{\partial \varepsilon}{\partial t} + u_j \frac{\partial \varepsilon}{\partial x_j} = \frac{\partial}{\partial x_j}\left[\left(v + \frac{v_t}{\sigma_\varepsilon}\right)\frac{\partial \varepsilon}{\partial x_j}\right] + (C_{1\varepsilon}G - C_{2\varepsilon}\varepsilon)\frac{\varepsilon}{k} \tag{28}$$

where u_i= averaged velocity field; x_i= Cartesian coordinate component; f_i= body force; p= pressure; $\tau_{ij} = -\rho\overline{u_i' u_j'}$, Reynolds stress, where u_i' is the fluctuating velocity field; k= turbulence kinetic energy; ε = dissipation rate of k; G= turbulence production rate; the eddy viscosity $v_t = C_\mu k^2/\varepsilon$ and coefficients $C_\mu = 0.09$, $\sigma_k = 1.0$, $\sigma_\varepsilon = 1.3$, $C_{1\varepsilon} = 1.44$, $C_{2\varepsilon} = 1.92$. Despite its success in solving many engineering problems in practice, the k-ε model suffers from some inherent drawbacks such as the assumption of local isotropic turbulence. Nagata et al. (2005) found that the original model could be improved after introducing a quadratic relation between the Reynolds stress and the rate of strain.

4.3 Sediment transport and bed variation

Compared with researches on flow modeling, simulation of sediment transport is far lagged and involves much empiricism. Sediment is generally divided into bedload and suspended load. Since the adjustment of bedload transport process to the flow condition proceeds rapidly, the transport of bedload is usually modeled with empirical formulae. For example, the relation proposed by Ashida and Michiue (1971) is written as

$$\frac{q_{bm}}{\sqrt{sgd_m^3}} = 17 p_{bm}\tau_{*em}^{3/2}\left(1 - \frac{u_{*cm}}{u_*}\right)\left(1 - \frac{\tau_{*cm}}{\tau_{*m}}\right) \tag{29}$$

where subscript m= sediment size fraction (bed load fraction here); q_{bm}= bed load discharge; d_m= diameter of fraction m; p_{bm}= percentage of sediment size fraction m in the bed composition; $\tau_{*m}, \tau_{*cm}, \tau_{*em}$= dimensionless shear stress, critical shear stress and effective shear stress, respectively; u_{*cm}= critical friction velocity.

The local bed slope affects the sediment transport significantly. Van Rijn (1993) pointed out that the critical shear stress for the sediment entrainment and the transport rate should be corrected. He separated the local bed slope as a longitudinal slope and a transverse slope and introduced correction methods correspondingly. Zhang et al. (2006) believed that the separation of the local bed slope into two slopes was physically unreasonable and derived a correction method in 3D directly. Moreover, unrealistic bed slope over the angle of sediment repose should be avoided in the simulation. Zhang et al. (2006) introduced a method to correct bed slope at the end of each time step. The method guaranteed that the bed slope was not greater than the angle of sediment repose as well as ensured that sediment conservativeness was maintained. Sekine (2004) and Nagata et al. (2005), however, assumed an *ad hoc* sediment transport rate due to a sliding process. They included the sediment transport rate in the bed deformation model instead of correcting the local bed slope after the bed deformation model was solved.

Suspended sediment is usually solved from the advection-diffusion equation as follow.

$$\frac{\partial C_m}{\partial t} + (u_j - w_{sm}\delta_{j3})\frac{\partial C_m}{\partial x_j} = \frac{\partial}{\partial x_j}\left[\left(\frac{v_t}{\sigma_c}\right)\frac{\partial C_m}{\partial x_j}\right] \tag{30}$$

where C_m= volumetric sediment concentration;

w_{sm} = sediment settling velocity for each fraction; σ_c = turbulent Schmidt number and δ_{ij} = Kronecker delta. The suspended load layer exchanges with the bedload layer via upward and downward fluxes and hence influences the bed topography and composition.

As is known, it takes time and space for sediment transport to adapt to its possible capacity under the specific local flow conditions. The non-equilibrium transport of sediment load around spur dykes has been reported by some researchers (e.g. Michiue and Hinokidani, 1992 and Nagata et al., 2005). Since most bedload transport formulae give transport rate under equilibrium condition, the results are questionable. There are two alternatives in the literature: introducing a non-equilibrium adaptation coefficient to account for the difference between the actual sediment transport and the prevailed transport under equilibrium condition (e.g. Minh Duc, et al., 2004), or employing stochastic models for sediment pickup and deposition (e.g. Onda et al., 2007).

When the sediment transport rate is known, the bed deformation is generally solved from the sediment continuity equation in the bedload layer. In a stochastic model, however, Nagata et al. (2005) obtained the temporal change of the bed level from the volumes of pickup and deposition.

4.4 Solution methods

To date, the FVM (Finite volume method) is the commonplace in CFD simulations. In an FVM, the governing equations are integrated over a series of CVs (Control volumes) covering the study domain instead of being solved directly. The mesh data for CVs may be organized in a structured way or an unstructured way. Structured mesh is very efficient for domains with relatively simple geometries (Bhuiyan et al., 2004). With the increasing of the geometry complexity, more suitable mesh system such as the boundary-fitted mesh may be employed (e.g. Onda et al., 2007). With a boundary-fitted mesh, some additional terms are introduced and governing equations may become very complex. However, boundary-fitted mesh still belongs to structured mesh and it may take full use of computational techniques developed for structured mesh. For most problems of engineering interest, an unstructured mesh system is promising, which provides an accurate resolution of complex geometries and boundaries as well as allows mesh adaptation (e.g. Zhang, 2005 and Zhang et al., 2006).

5. Suggestions for future researches

Although there have been great achievements on scour around spur dykes over the past years, a lot of challenges remain for future researches.

The deposition and erosion of nonuniform sediment have significant influence on the scour process and are closely related to riverine habitat. But the progress is very slow in developing reliable predictive tools mainly due to the shortage of scientific knowledge in bed sorting mechanisms and high-quality experiment or field data. Since sediment particles in actual rivers generally cover a wide spectrum of sizes, this is a research field to be explored urgently.

The effect of the groundwater pore pressure on the scour process deserves special attention as well. The gradient of the pore pressure during the drawdown of a flood or tsunami may cause significant reduction in the effective shear stress in the substrate and therefore enhanced scour (Sumer, 2008). Transient scour may develop rapidly behind a spur dyke when there is a sudden change in the ground water level. This phenomenon may result in the undermining of the spur dyke and a degradation of the pool habitat around the spur dyke. Therefore, incorporating ground water in the morphological model is a new challenge and of great value.

Up to now, sediment transport has been correlated with the mean flow and near-bed shear stress. However, this concept is found to be not sufficient for quantitatively accurate prediction of scour (Chrisoholdes, et al., 2003). The importance of the turbulent coherent structure on sediment threshold and transport has been pointed out by some researchers such as Gyr and Hoyer (2006). An entire image of the scour process necessitates a breakthrough in linking the understanding at small scales such as the micromechanics of flow and sediment transport to large scales such as vortex systems and bed deformation in laboratory flumes and actual rivers.

References

Ahmad, M. (1953): Experiments on design and behavior of spur dikes, Proc. IAHR Convention, Minnesota, pp. 145-159.

Ashida, K. and Michiue, M. (1972): Studies on bed load transportation for nonuniform sediment and river bed variation, Annuals of DPRI, Kyoto Univ., No. 14B, pp. 259-273. (in Japanese)

Bhuiyan, ABM F., Huque, F. and Saifuddin, AKM (2004): Numerical modeling of flow pattern & bed evolution around spur-type structures, Proc. 9th Int. Symp. on Riv. Sed., Yichang, pp. 1497-1502.

Cao, Z. and Carling, P. (2001): Mathematical modeling of alluvial rivers: reality and myth. Part 1: general review, Water & Maritime Eng., ICE, Vol. 154, No. 3, pp. 207-219.

Cardoso, A.H. and Bettess, R. (1999): Effects of time & channel geometry on scour at bridge abutments, J. Hydraul. Eng., ASCE, Vol. 125, No. 4, pp. 388-399.

Chabert, J. and Engeldinger, P. (1956): Etude des afouillements autour des piles des ponts, Laboratoire National d'Hydraulique, Chatou, France. (in French)

Chen, F.Y. and Ikeda, S. (1997): Horizontal separation flows in shallow open channels with spur dikes, J. Hydrosci. & Hydraul. Eng., JSCE, Vol. 15, No. 2, pp. 15-30.

Chiew, Y.M. (1984): Local scour at bridge piers, Report No. 355, Univ. of Auckland, School of Eng., New Zealand.

Chin, C.O., Melville, B.W. and Raudkivi, A.J. (1994): Streambed armoring, J. Hydraul. Eng., ASCE, Vol. 120, No. 8, pp. 899-918.

Chrisoholdes, A, Sotiropoulos, F. and Strum, T.W. (2003): Coherent structures in flat-bed abutment flow: computational fluid dynamics simulations and experiments, J. Hydraul. Eng., ASCE, Vol. 129, No. 3, pp.177-186.

Coleman, S.E., Lauchlan, C.S. and Melville, B.W. (2003): Clear-water scour development at bridge abutments, J. Hydraul. Res., IAHR, Vol. 41, No. 5, pp. 521-531.

Dey, S. and Barbhuiya, A.K. (2004): Clear-water scour at abutments in thinly armored beds, J. Hydraul. Eng., ASCE, Vol.130, No.7, pp.622-634.

Dey, S. and Barbhuiya, A.K. (2005): Time variation of scour at abutments, J. Hydraul. Eng., ASCE, Vol. 131, No. 1, pp.11-23.

Garde, R.J., Subramanya, K. and Nambudripad, K.D. (1961): Study of scour around spur-dikes, J. Hydraul. Div., Proc. ASCE, Vol. 87, No. HY6, pp. 23-37.

Gill, M.A. (1972): Erosion of sand beds around spur dikes, J. Hydraul. Div., Proc. ASCE, Vol. 98, No. HY9, pp. 1587-1602.

Gyr, A. and Hoyer, K. (2006): Sediment Transport: a Geophysical Phenomenon, Springer.

Ho, J., Yeo, H.K., Coonrod, J. and Ahn, W.S. (2007): Numerical modeling study for flow pattern changes induced by single groyne, 32nd Congress of IAHR, Venice, Italy, CD-ROM.

Inglis, C.C. (1949): The behaviour and control of rivers and canals, C.W.I.N.R.S. Poona, Res. Pub. No. 13.

Ishigaki, T. and Baba, Y. (2004): Local scour induced by 3D flow around attracting & deflecting groins, Proc. 2nd Int. Conf. on Scour and Erosion, Meritus Mandarin, Singapore, pp. 301-308.

Johnson, P.A. and Dock, D.A. (1998): Probabilistic bridge scour estimates, J. Hydraul. Eng., ASCE, Vol. 124, No. 7, pp. 750-754.

Kimura, I. and Hosoda, T. (1997): Fundamental properties of flows in open channels with dead zone, J. Hydraul. Eng., ASCE, Vol. 123, No. 2, pp. 98-107.

Kimura, I., Hosoda, T. and Onda, S. (2002): Prediction of 3D flow structures around skewed spur dikes by means of a non-linear k-ε model, RiverFlow 2002, Bousmar & Zech (eds), Balkema, Vol. 1, pp. 65-73.

Kinki Regional Development Bureau, MLIT, Japan (2002): Lake Biwa & the Yodo River.

Kothyari, U.C. and Ranga Raju, K.G. (2001): Scour around spur dikes and bridge abutments, J. Hydraul. Res., IAHR, Vol. 39, No. 4, pp. 367-374

Kothyari, U.C., Garde, R.J. and Ranga Raju, K.G. (1992): Temporal variation of scour around circular bridge piers, J. Hydraul. Eng., ASCE, Vol.

118, No. 8, pp. 1091-1106.

Kuhnle, R.A., Alonso, C.V. and Shields Jr., F.D. (1999): Geometry of scour holes associated with 90° spur dyke, J. Hydraul. Eng., ASCE, Vol. 125, No. 9, pp.972-978.

Kuhnle, R.A., Alonso, C.V. and Shields Jr., F.D. (2002): Local scour associated with angled spur dyke, J. Hydraul. Eng., ASCE, Vol. 128, No. 12, pp.1087-1093.

Lausen, E.M. (1960): Scour at bridge crossing, J. Hydraul. Div., Proc. ASCE, Vol. 86, No. HY2, pp. 39-54.

Lausen, E.M. (1963): Analysis of relief bridge scour, J. Hydraul. Div., Proc. ASCE, Vol. 89, No. HY3, pp. 93-118.

Lim, S.Y. (1997): Equilibrium clear-water scour around an abutment, J. Hydraul. Eng., ASCE, Vol. 123, No. 3, pp. 237-243.

Lim, S.Y. and Cheng, N.S. (1998): Prediction of live-bed scour at bridge abutment, J. Hydraul. Eng., ASCE, Vol. 124, No. 6, pp. 635-638.

Liu, J., Tominaga, A and Nagao, M. (1994): Numerical simulation of the flow around the spur dikes with certain configuration and angles with bank, J. Hydrosci. & Hydraul. Eng., JSCE, Vol. 12, No. 2, pp. 85-100.

Marson, C., Caroni, E., Fiorotto, V. and Da Deppo, L. (2003): Flow field analysis around a groyne, 31st IAHR Congress, Thessaloniki, Greece, Vol. 2, pp. 377-384.

Mayerle, R., Toro, F.M. and Wang, S.S.Y. (1995): Verification of a three-dimensional numerical model simulation of the flow in the vicinity of spur dikes, J. Hydraul. Res., IAHR, Vol. 33, No. 2, pp. 125-136.

Melville, B.W. (1992): Local scour at bridge abutments, J. Hydraul. Eng., ASCE, Vol. 118, No.4, pp. 615-631.

Melville, B.W. (1995): Bridge abutment scour in compound channel, J. Hydraul. Eng., ASCE, Vol. 121, No. 12, pp.863-868.

Melville, B.W. (1997): Pier and abutment scour: integrated approach, J. Hydraul. Eng., ASCE, Vol. 123, No. 2, pp.125-136.

Melville, B.W. and Sutherland, A.J. (1988): Design method for local scour at bridge piers, J. Hydraul. Eng., ASCE, Vol. 114, No. 10, pp. 1210-1226.

Michiue, M. and Hinokidani, O. (1992): Calculation of 2-dimensional bed evolution around spur-dike, Annual J. Hydraul. Eng., JSCE, Vol. 36, pp. 61-66. (in Japanese)

Michiue, M., Suzuki, K. and Hinokidani, O. (1984): Formation of low-water bed by spur-dikes in alluvial channels, Proc. 4th APD-IAHR Congress.

Minh Duc, B., Wenka, T. and Rodi, W. (2004): Numerical modeling of bed deformation in laboratory channels, J. Hydraul. Eng., ASCE, Vol. 130, No. 9, pp. 894-904.

Molinas, A., Kheireldin, K. and Wu, B. (1998): Shear stress around vertical wall abutments, J. Hydraul. Eng., ASCE, Vol. 128, No., pp. 811-820.

Muto, Y., Imamoto, H. and Ishigaki, T. (2000): Turbulence Characteristics of a shear flow in an embayment attached to a straight open channel, Proc. 4th Int. Conf. on Hydrosci.& Eng., Seoul, Korea, pp.232-240.

Nagata, N., Hosoda, T. Nakato, T. and Muramoto, Y. (2005): Three-dimensional numerical model for flow and bed deformation around river hydraulic structures, J. Hydraul. Eng., ASCE, Vol. 131. No. 12, pp. 1074-1087.

Nakagawa, H., Zhang, H., Ishigaki, T. and Muto, Y. (2004): Prediction of 3D flow field with non-linear k-ε model based on unstructured mesh, J. Appl. Mech., JSCE, Vol. 7, pp. 1077-1088.

Nakagawa, K. Kawahara, Y. and Tamai, N. (1995): Experimental study on hydraulic characteristics of flows in embayments, Annual J. Hydraul. Eng., JSCE, Vol. 39, pp. 595-600. (in Japanese)

Onda, S., Hosoda, T. Kimura, I. and Iwata, M. (2007): Numerical simulation on local scouring around a spur dyke using equilibrium and non-equilibrium sediment transport models, Annual J. Hydraul. Eng., JSCE, Vol. 51, pp. 943-948. (in Japanese)

Ouillon, S. and Dartus, D. (1997): Three-dimensional computation of flow around groyne, J. Hydraul. Eng., ASCE, Vol. 123, No. 11, pp. 962-970.

Peng, J. and Kawahara, Y. (1998): Application of linear and non-linear k-ε models to flows around spur dykes, Annual J. of Hydraul. Eng., JSCE, Vol. 42, pp. 643-648.

Raudkivi, A.J. and Ettema, R. (1983): Clear-water scour at cylindrical piers, J. Hydraul. Eng., ASCE, Vol. 109, No. 3, pp. 338-350.

Sekine, M. (2004): Numerical simulation of braided stream formation on the basis of slope-collapse model, J. Hydrosci. & Hydraul. Eng., JSCE, Vol. 22, No. 2, pp. 1-10.

Shields, F.D.Jr. Cooper, C.M. and Knight, S.S. (1995): Experiment in stream restoration, J. Hydraul. Eng., ASCE, Vol. 121, No. 6, pp. 494-502.

Sturm, T.W. and Janjua, N.S. (1993): Clear-water scour around abutments in floodplains, J. Hydraul. Eng., ASCE, Vol. 120, No. 8, pp. 956-972

Sumer, B.M. (2007): Mathematical modeling of scour: a review, J. Hydraul. Res., IAHR, Vol. 45, No. 6, pp. 723-735.

Suzuki, K. (1989): Hydraulic functions & problems of river training structures, JSCE Summer Course in Hydraul. Eng., pp. A-4-4-A-4-22. (in Japanese)

Tison, Jr. G. (1962): Discussion on Study of scour around spur-dikes, J. Hydraul. Div., Proc. ASCE, Vol. 88, No. HY4, pp. 301-306.

Tominaga, A. and Matsumoto, D. (2006): Diverse riverbed figuration by using skew spur-dike groups, RiverFlow 2006, Lisbon, pp. 683-691.

Uijttewaal, W.S.J. (1999): Groyne field velocity patterns determined with particle tracking velocimetry, 28th IAHR Congress, Graz, Austria.

Uijttewaal, W.S.J., Lehmann, D. and van Mazijk, A. (2001): Exchange processes between a river and its groyne fields: model experiments, J. Hydraul. Eng., ASCE, Vol. 127, No. 11, pp. 928-936.

Van Rijn, L.C. (1993): Principles of Sediment Transport in Rivers, Estuaries and Coastal Seas, AQUA Publications.

Yeo, H.K. (2007): Nature-friendly river-training structure using groynes, the 4th Joint Seminar between IWHR-KICT, July 9, Beijing.

Yossef, M.F.M. and Klaassen, G.J. (2002): Reproduction of groyne-induced river bed morphology using LES in a 2-D morphological model, RiverFlow 2002, Bousmar & Zech (eds), Balkema, pp. 1099-1108.

Zhang, H. (2005): Study on flow and bed deformation in channels with spur dykes, Doctoral Dissertation, Kyoto Univ.

Zhang, H. and Nakagawa, H. (2008): Investigation on morphological consequences of spur dyke with experimental and numerical methods, Proc. 8th Int. Conf. on Hydrosci. & Eng., Nagoya. (to appear)

Zhang, H., Nakagawa, H., Ishigaki, T. and Muto, Y. (2004): Prediction of 3D flow field and local scouring around spur dykes, Annual J. Hydraul. Eng., JSCE, Vol. 49, pp. 1003-1008.

Zhang, H., Nakagawa, H., Ishigaki, T., Muto, Y. and Khaleduzzaman, A.T.M. (2005): Flow & bed deformation around a series of impermeable & permeable spur dykes, Proc. Int. Conf. on Monitoring, Prediction and Mitigation of Water-related Disasters, Kyoto, pp. 197-202.

Zhang, H., Nakagawa, H., Muto, Y., Baba, Y. and Ishigaki, T. (2006): Numerical simulation of flow and local scour around hydraulic structures, River Flow 2006, Lisbon, pp. 1683-1693.

水制周辺の局所洗掘に関する研究：進展と展望

張　浩・中川　一

要　旨

　水制周辺の局所洗掘は一般的な水理現象であるものの，課題の多い研究テーマである。局所洗掘が人間にとって利益となるか災害となるかは，洗掘の過程が十分に解明され効果的に管理されているかどうかに依存するため，長年にわたって研究され，多くの関心を集めてきた。本論文では関連する研究の背景および展望について報告する。論文は三つの部分から構成される。まず，水制周辺流れの特性，最大洗掘深の予測，洗掘の時・空間的変化特性，水制群による洗掘に関する研究の現状を概観する。次に，モデル構築の基本原則，支配方程式，数値計算方法を含めた数値シミュレーション技術の進展について述べる。最後に，将来の研究方向をいくつか提示する。

キーワード:水制，局所洗掘，進展，展望